ELSEVIER

Biochimica et Biophysica Acta 1280 (1996) 161–168

BBA Biochimica et Biophysica Acta

Role of membrane fluidity in Epstein Barr virus (EBV) infectivity on Akata cell line

D. Pozzi [a], A. Lisi [b], G. Lanzilli [b], S. Grimaldi [b,*]

[a] *Dipartimento di Medicina Sperimentale e Patologia, Università 'La Sapienza' Roma, Roma, Italy*
[b] *Istituto di Medicina Sperimentale, C.N.R., Viale Marx 43, 00137 Roma, Italy*

Received 24 July 1995; revised 15 November 1995; accepted 30 November 1995

Abstract

Infection of Epstein Barr virus (EBV) to its host cells is initiated by the attachment of the glycoprotein gp 350/220 to the CR2 molecule. We used the sensitivity at the polar environment of the fluorescent probe Laurdan to study the membrane viscosity distribution from single leaving cells on two lymphoid cell lines Raji and Akata. Lipid analysis on both cells line demonstrated a lower cholesterol to phospholipid molar ratio on Akata than Raji cells. Cell fluidity analysis by Laurdan generalized emission polarization (GP) or by DPH polarization, indicated that membrane viscosity of Akata was lower than Raji cells. This difference was correlated to the increased susceptibility of Akata cells in expressing EBV early antigens (EA) after EBV superinfection.

Keywords: Epstein Barr virus; Membrane fluidity; Laurdan

1. Introduction

Epstein Barr virus (EBV) is a human herpes virus etiologically linked to infectious mononucleosis and closely associated with at least two human malignancies, Burkitt's lymphoma and nasopharyngeal carcinoma [1,2]. EBV can infect human B lymphocytes in vitro; cells became immortalized and the viral genome persists in infected cells in a latent state [3]. We have shown that calcium modulation activates the viral genome in vitro, leading to induction of viral antigen expression and that this event is mediated by activation of cellular protein kinase C (PKC) [4–6]. Superinfection of latently infected cells can also induce within few hours early antigen (EA) production [7]. The EBV receptor, the CR2 molecule, is a 145 kDa glycoprotein also known as the receptor for the C3d fragment of the complement [8,9]. The major EBV envelope glycoprotein gp 350/220 binds to CR2 [10,11], virus fusion is then mediated by a third viral glycoprotein, the gp 85 protein, that allowed the virus to enters cells either by direct fusion or receptor mediated endocytosis, depending on the cell type [12,13]. For virus cell membrane fusion to occur, the apposing membrane bilayers have to undergoes structural changes leading to lipid rearrangements and deformations. A numbers of lipids including cholesterol and its hydrophilic ester cholesterol hemisuccinate, can modulate membrane fusion through changes in membrane fluidity [15]. It has recently been suggested [16] that the inability of EBV to fuse with some CR2 positive cell line could be related to specific lipid composition of the plasma membrane. To better understand the role of cell membrane composition in the first steps of EBV entry into lymphoid cells, we used the fluorescent membrane probes Laurdan and DPH. Laurdan is located at the hydrophilic/hydrophobic interface of the membrane bilayer [17,18] with the lauric acid tail anchored in the phospholipid acyl chain region, and is known to be sensitive to the polarity of the environment, displaying a large red shift of the emission in polar solvent with respect to non polar solvents [19]. Parasassi [20] demonstrated that is possible by Laurdan emission spectroscopy to quantitate both the relative amount of gel (blue emission 435 nm) and liquid crystalline phases (red emission 490 nm). They also suggested that the quantitation of the phases can be obtained using

Abbreviations: gp, glycoprotein; GP, generalized polarization; CR2, complement receptor type 2; EA, early antigens; DPH, diphenylexathriene; R18, octadecyl rhodamine B chloride; bisindolylmaleimide, 2-(1-(3-dimethylaminopropyl)-1H-indol-3-yl)-3-(1H-indol-3-yl)-maleimide; PKC, protein kinase C; PS, phosphatidylserine.

* Corresponding author. Fax: + 39 6 86090332.

SSDI 0005-2736(95)00289-8

steady-state generalized polarization (GP). They define 'generalized polarization' to be

$$GP = I_{blue} - I_{red}/I_{blue} + I_{red} \quad (1)$$

Fluorescence microscopy, to study membrane fluidity by fluorescence polarization measurements, has not been used so far due to technical and physical problems related to the use of polarizers. We successfully used Laurdan to monitor membrane fluidity in fluorescence microscopy thanks to the sensitivity of this probe to the polarity of microenvironment. Fluorescence microscopy, with respect to steady state measurements, has less variation due to cell population heterogeneity. Laurdan is a membrane probe that can be utilized to study membrane fluidity by fluorescence emission instead of fluorescence emission polarization, thus enabling us to study membrane fluidity by fluorescence microscopy on single cells to better define the early stages of EBV replication. In the present work we correlate membrane fluidity and disruption of EBV latency in Akata cells, we also attempted to quantify single cell membrane fluidity, using the fluorophore Laurdan.

2. Materials and methods

2.1. Materials

Octadecylrhodamine B chloride (R18) and 6-dodecanoyl-2-dimethylaminonaphtalene (Laurdan) were obtained from Molecular Probes (Junction City, OR), Triton X-100 from Aldrich, TPA from Sigma, [γ-^{32}P]ATP (3000 Ci/mmol) from Amersham, bisindolylmaleimide from Calbiochem.

2.2. Cell cultures

Raji and Akata cells were grown in RPMI (Gibco Laboratories, UK) supplemented with 10% Fetal Calf Serum (Gibco Laboratories, UK) and antibiotics (110 IU/ml of penicillin and 100 μg/ml of streptomycin) at 37°C, 5% CO_2. All this cells line are EBV genome-positive which express CR2.

2.3. Virus production

P3HR1 virus was harvested from the spent supernatant of P3HR1 cells grown for 14 days at 37°C, clarified by centrifugation (2000 × g, 15 min). The virus was pelleted at 20 000 × g for 90 min. Pellets were suspended in 1/250 of the original volume and filtered through a 0.45 μm pore filter.

2.4. Lipid phosphate analysis

Lipid phosphate analysis was performed using the molybdate-ascorbate method as previously reported [21].

2.5. Cholesterol analysis

Cholesterol content of the extracted lipids was determined using the colorimetric method of Zlatkis et al. [22] An aliquot of the chloroform solution containing cellular lipids was evaporated under nitrogen stream. Than the dried lipids were acidified with acetic acid and vortexed vigorously. Two ml of diluted color reagent (2.5 g $FeCl_3 \cdot 6H_2O$/100 ml of 85% orthophosphoric acid diluted 1:12.5 with concentrated sulfuric acid) was added to the tubes and the content were gently mixed. Than absorbance was read at 550 nm.

2.6. Cholesterol enrichment

Cholesterol enrichment of Raji and Akata cells membrane has been performed using PVP complexed with BSA described by Shinitzky et al. [23] and modified by Patel et al. [24]. The complex was prepared as follows: 3.5% PVP in PBS was dialyzed overnight and cholesterol was added to provide a final concentration of 260 nmol.

2.7. In vitro phosphorylation

Raji and Akata cells ($5 \cdot 10^6$), native or cholesterol enriched, were rinsed with Locke's solution (154 mM NaCl, 5.6 mM KCl, 3.6 mM $NaHCO_3$, 2.3 mM $CaCl_2$, 5.6 mM glucose, 5 mM Hepes, pH 7.4) containing 1 mM $MgCl_2$. Labeling was carried out in 100 μl Locke's solution containing 0.4 mM $MgCl_2$ and 0.3 mCi/ml [^{32}P]orthophosphate for 45 min at room temperature on a rocker. The PKC inhibitor Bisindolylmaleimide (0.5 μM) were added to the cultures 30 min prior to stimulation with TPA/Butirrate. At various time points cells were briefly rinsed with (2 × 0.5 ml) Locke's solution and collected with (3 × 0.25 ml) chilled cell lysis buffer (1 mM $MgCl_2$, 0.5 mM EGTA, 0.5 mM dithiothreitol (DTT), 2% pyrophosphate, 5 mM Tris-Cl, pH 7.4). Ice-cold trichloroacetic acid (TCA) was quickly added to the lysates (20% (w/v) final) and after incubation on ice for 30 min, precipitates were collected by centrifugation. Pellets were resuspended in 50 μl of SDS sample buffer (9 M urea, 0.14 M β-mercaptoethanol, 0.04 M DTT, 2% SDS, 0.075 M Tris-Cl, pH 8.0) and boiled for 5 min. (25)

2.8. Electrophoresis

SDS-polyacrylamide gel electrophoresis (SDS-PAGE) was carried out according to Laemmli [26]. Equal volumes of sample (20 μl/well) were loaded. Two-dimensional gel electrophoresis was carried out in according to [25]. Equal volumes of samples (11 μl/well) were loaded. The first dimensional non equilibrium isoelectric focusing gels (1.8 × 75 mm) containing a 3% total carrier ampholytes mixture composed of 75% pH 3.5–9.5, 25% pH 5.0–8.0, 9 M urea, 0.5% Nonidet P-40, 1.6% 3-(3-cholamidopropyl)di-

methylammonio)-1-propanesulfonate (Chaps), 5% acrylamide were run for 1500 Vh; the second dimension was carried out on 6–14% SDS polyacrylamide gradient gel. Incorporation of ^{32}P label was revealed by autoradiography and, in two-dimensional gels, quantitated with a Phosphorimages Densitometer (Molecular Dynamics).

2.9. Protein kinase C assay

Cytosol and membrane fractions were adsorbed in a 1.5 ml microcentrifuge tube to a 0.2 ml of DEAE-Sepharose fast flow equilibrated in buffer A (20 ml Hepes, pH 7.5–10 mM β-mercaptoethanol-0.5 mM EDTA-0.5 mM EDTA), washed three times with buffer A and eluted with 0.2 M NaCl in buffer A. The 0.2 M NaCl eluate were incubated in a 50 μl reaction mixture containing 20 mM Tris-HCl (pH 7.5), 10 mm $MgCl_2$, 40 μg of histone H_1, 100 μg/ml of PS, 500 μM $CaCl_2$ or 200 μM EGTA in place of $CaCl_2$ and PS. Assays were carried out as previously reported [14].

2.10. Virus fusion assay

P3HR1 virus was labeled with R18 as described previously [27]. R18-P3HR1 was preincubated with Raji and Akata cells at 4°C for 30 min to form virus-cells complex and unbound virus was removed by centrifugation in a 12 × 75-mn polystyrene tube at 330 × *g*. The pellet containing the complex was resuspended in phosphate buffer and kept on ice. 50 μl of the complex were added to 2 ml of buffer prewarmed at 37°C. Percentage of fluorescence dequenching (%FDQ) was calculated according to Eq. 2:

$$\%FDQ = (F - F_0/F_t - F_0) \times 100 \quad (2)$$

were F_0 and F are the fluorescence intensity at time 0 and at given point, F_t is the fluorescence after Triton addition.

2.11. Laurdan labeling of cell membrane

Laurdan labeling procedure is according to Parasassi et al. [28]. $1 \cdot 10^6$ of each cells type were washed three times with PBS, then resuspended in 2.5 ml of PBS. 0.5 μl of a 2.5 mM solution of Laurdan in DMSO were added to cell suspension under mild magnetic stirring. Incubation were carried out in the dark for 20 min. Cells were than pelleted and washed with PBS, resuspended in 2.5 ml of PBS, equilibrated for 5 min in the fluorescence microscope at 20°C, than measured. These labeling conditions were determined after dilution experiments, where the GP value was reported as a function of the ratio (10^6 cell per ml/(mol Laurdan) (C/L). Since Laurdan can diffuse from the plasma membrane to intracellular membranes each set of cells (50 to 70 cells) were analyzed within 10 min. Within this time frame only the plasma membrane appears fluorescent when laurdan is excited at 360 nm under the epifluorescence microscope. Each experiment repeated up to 10 times.

2.12. Generalized polarization measurements

Single cell Laurdan emission fluorescence were obtained using an Olympus BH2 epifluorescence microscope equipped with a photo tube and a special software (ISS Inc., Champaigne, IL). The microscope was equipped with photon counting electronics PX01 (ISS). the Excitation (360 nm) and emission (435/490) filters (Corning) bandpass were 5 nm. The emission were corrected for the lamp intensity variation. GP values using 360 nm as excitation wavelength were obtained from Eq. 2:

$$GP = I_{435} - I_{490}/I_{435} + I_{490}$$

where I_{435} and I_{490} are the intensities at each wavelength. In some experiment Laurdan excitation and emission spectra were recorded using a Perkin-Elmer 650-40 spectrofluorometer using a xenon lamp as the light source and the accompanying software (ISS, Urbana Champaign, IL).

2.13. Fluorescence polarization measurements

1,6-Diphenyl-1,3,5-hexatriene (DPH) (Sigma) and 1,2-trimethylamino-6-phenylexa-1,3,5-triene (TMA-DPH) (Sigma), a cationic analog of DPH, were used for monitoring the fluidity in the hydrocarbon core and the exofacial leaflet of the plasma membrane, respectively [24]. Labeling of intact cells was performed by adding 2 μl of 1 mM DPH in tetrahydrofuran or TMA-DPH in dimethylsulfoxide to 40 μg of protein/ml. Than incubated in the dark at 4°C for 60 min. Fluorescence polarization was measured using a Perkin Elmer 650-40 spectrofluorometer. The degree of fluorescence polarization P, defined in the following equation was directly recorded.

$$P = I_v - I_h/I_v + I_h$$

I_v and I_h are the emission intensities when the polarizers are oriented vertically and horizontally, respectively.

2.14. Early Antigens (EA) detection

After 72 h from cell superinfection or induction, cells were analyzed for EBV EA production by the indirect immunofluorescent test [5]. Cells were first fixed at −20°C in acetone than incubated for 30 min at 37°C with human anti EA MoAb. After extensive washing cells were incubated with a fluoresceinated secondary antibody, than EA analysis was carried out using an epifluorescence microscope and the results expressed as % EA positive cells.

2.15. Flow cytometer analysis of CR2 molecule

Cells from culture were washed in PBS and fixed in 2% paraformaldehyde. For indirect immunofluorescence, 50

Table 1
CR2 and EA expression on Raji and Akata cells

Cells type	%CR2	%EA
Raji	90	7.5
Akata	20	25

EA were detected in Raji and Akata cells after EBV superinfection and expressed as %EA positive cells by the indirect immunofluorescent assay. CR2 were quantitated in control Raji and Akata cells by flow cytometry analysis as described under Section 2.

μl of cell suspension with approx. 10^6 cells were incubated with 20 μl anti-CR2 MoAb for 30 min on ice, then washed and resuspended in 50 μl of PBS. 4 μl of fluoresceinated secondary antibody were added and the cells incubated at 4°C in the dark for 30 min. Cells were resuspended in 200 μl PBS and kept on ice until FACS analysis. For negative controls the cells were incubated only with the secondary antibody. Fluorescence was detected using a FACScan Flow Cytometer (Becton Dickinson) equipped with air-cooled Argon-ion laser emitting at 488 nm and single parameter histograms were collected for green fluorescence.

3. Results

3.1. CR2 and EA expression on Raji and Akata cells

Akata cells EBV superinfected proved to be more susceptible to EA production compared to Raji cells. The higher susceptibility of Akata is, to some extent, surprising since by FACS analysis of CR2 molecule, those cells are less positive than Raji (Table 1). Incubation of R18 labeled EBV with Akata resulted in a higher R18 fluorescence dequenching than found with Raji. The amount of EBV bound to both cell lines has been quantified (data not shown) by measuring the fluorescence after Triton X-100 addition, providing a relative measure of the amount of virus bound that, for Akata, was 70% less than what found for Raji cells. Despite EBV binds to less extent to Akata, the virus fuses and penetrate better with this cells than Raji (Fig. 1).

3.2. Lipids and cholesterol profile of Raji and Akata cells

To determine if the difference in the ability of EBV to fuse and induce EA with Akata compared to Raji cells might be related to difference in cell membrane lipids, as already reported for other cell types [16], lipid and cholesterol analysis was performed on both cell types. Both cell lines contained similar amount of cholesterol expressed per mg of cell protein (Table 2). Phospholipids phosphate analysis, showed that Akata cells had more phospholipid phosphate per mg of protein, resulting in a lower cholesterol/phospholipid molar ratio of Akata compared to Raji cell membranes.

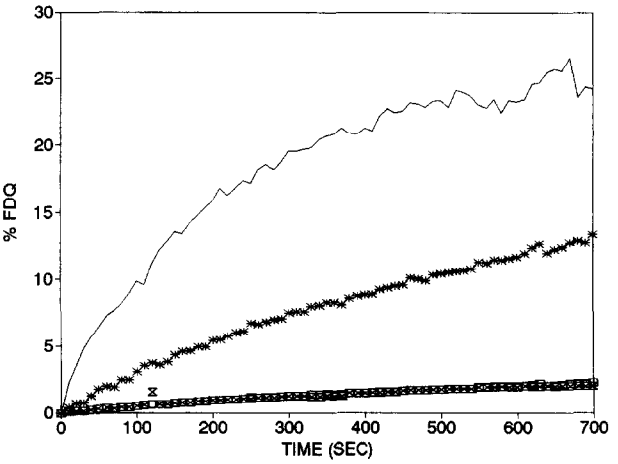

Fig. 1. Effect of cholesterol on the kinetics of EBV entry in Akata and Raji cells. $2 \cdot 10^6$/ml cells were incubated with R18EBV for 1 h at 4°C. Fusion was then followed for Akata (—), Akata cholesterol enriched (⋈), Raji (*) and Raji cholesterol enriched (□) using 560 and 590 nm as excitation end emission wavelengths, respectively. Data are expressed as % of R18 fluorescence dequenching after Triton X-100 addition.

3.3. Membrane cholesterol and kinetics of EBV fusion with Raji and Akata cells

To understand, to some more extent, the correlation between Akata and Raji cell membrane composition and EBV fusion, we attempted to modify cell membrane composition. Incubation of Akata and Raji cells with cholesterol-hemisuccinate dramatically changed the cholesterol/phospholipid molar ratio of Akata and Raji from 0.15 and 0.21 to 0.40 cholesterol/phospholipid molar ratio. The effect of this increase on Akata and Raji membrane cholesterol on their ability to fuse with R18 labeled EBV is reported in Fig. 1. Cholesterol incorporation on Akata and Raji cells membranes resulted in the abolishment of the ability of the labeled virus to fuse with the cholesterol enriched membrane compared to control cells.

3.4. Laurdan generalized emission polarization of Raji and Akata cell membranes

Measuring fluorescence from single cells by fluorescence microscopy offers the advantage to studying fluorescence distribution compared to the average number ob-

Table 2
Cholesterol and phospholipid content

Source	Cholesterol (nmol/mg protein)	PO_4 (nmol/mg protein)	Cholesterol/phospholipids (molar ratio)
Raji	20.6	100	0.21
Akata	23	156	0.15

Lipids determination were carried out using total lipid extracts as described under Section 2.

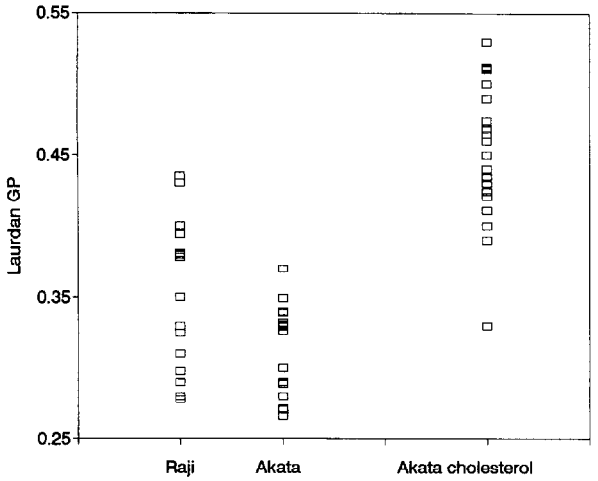

Fig. 2. Effect of cholesterol enrichment on Laurdan generalized emission polarization of Akata cells. Cells were labeled with Laurdan as described under Section 2, than fluorescence were recorded on single leaving cell under a fluorescence microscope equipped with a photon counting using 360 nm as excitation and 435–490 nm for emission wavelengths. Data point represent the means of three separate experiments with duplicate readings at each temperature.

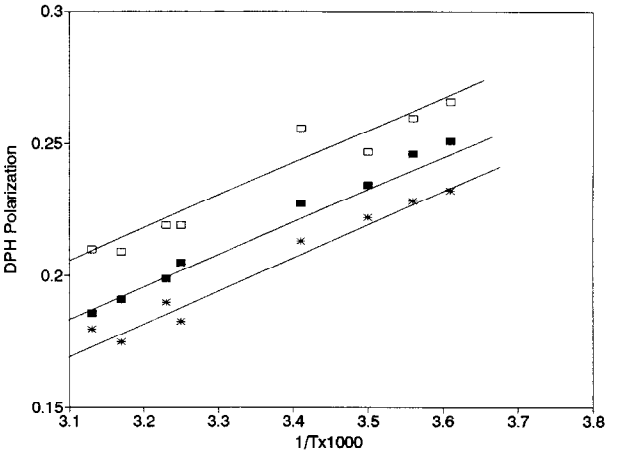

Fig. 3. Raji and Akata membrane fluidity by DPH fluorescence polarization. Effect of temperature on the fluorescence polarization of DPH in Akata (*), Akata cholesterol enriched (□) and Raji (■). Depicted is an Arrhenius plot of DPH polarization between 4 and 40°C. Data point represent the means of three separate experiments with duplicate readings at each temperature.

tained by steady state measurements under the light of a fluorescence spectrophotometer. Additionally, Laurdan is a suitable fluorescence probe to detect changes in membrane fluidity thanks to the sensitivity of its fluorescent emission spectra to the environment. This compared to other membrane probes, such as DPH, which utilize polarizers to detect changes in membrane fluidity, allowed Laurdan to be used in all the commonly equipped fluorescence microscopes. Single cell Laurdan emission GP from Raji and Akata generate for the first cell type two GP families equally represented, one ranging from GP = 0.35 to 0.45 the other ranging from 0.35 to 0.25. GP analysis from Akata cells identified only one family with GP distributed from GP = 0.35 to 0.25. Since higher GP values correspond to a more rigid membrane, one should expect that almost 50% of Raji cell population are characterized by a more rigid membrane than Akata (Fig. 2).

Labeling cholesterol enriched Akata cells with Laurdan and analyzing the GP values obtained from each single cells, resulted in a shift in each single cell emission GP values towards more rigid membranes, generating a family of points above ranging from GP = 0.35 to 0.55 (Fig. 2).

3.5. Membrane fluidity of Akata cells as measured by DPH

To investigate in further detail if the varying behavior towards EBV fusion of Akata compared to Raji cells could arise from difference in cell membrane fluidity, as suggested by single cell Laurdan emission GP, we analyzed membrane fluidity by steady-state DPH fluorescence polarization spectroscopy. Conversion of polarization values to apparent membrane microviscosity values, indicates that the membrane of Akata cells are significantly more fluid than Raji cells. Addition of cholesterol to reach a cholesterol/phospholipid molar ratio of 0.4 is acting as a rigidifier (Fig. 3).

3.6. Membrane fluidity of Akata cells as measured by TMA-DPH

The cationic DPH, TMA-DPH analog has spectral characteristic similar to those of the neutral parent probe DPH. The charged substituent in TMA-DPH provide a surface anchor improving the partition of the probe mainly in the cell plasma membrane [29]. As found in DPH polarization experiments, Akata cells plasma membrane demonstrated to be in a more fluid situation that Raji and cholesterol addition to Akata is acting as a rigidifier (Fig. 4).

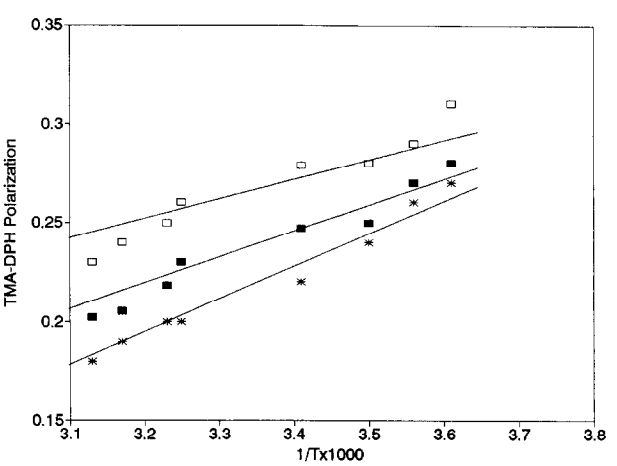

Fig. 4. Raji and Akata membrane fluidity by TMA-DPH fluorescence polarization. Effect of temperature on the fluorescence polarization of TMA-DPH in Akata (*), Akata cholesterol enriched (□) and Raji (■). Depicted is an Arrhenius plot of DPH polarization between 4 and 40°C. Data point represent the means of three separate experiments with duplicate readings at each temperature.

Table 3
Effect of membrane cholesterol on % EA expression by EBV superinfection on Raji and Akata cells

Cells type	%EA control		%EA cholesterol	
	no EBV	EBV	no EBV	EBV
Raji	2	7.5	2	2
Akata	4	25	3	2.5

After cholesterol enrichment EA were detected as in Table 1.

3.7. Membrane cholesterol and EA expression

Enrichment of both cell lines in membrane cholesterol, modulate the expression of EA after EBV superinfection. Incubation with cholesterol hemesuccinate followed by EBV induction resulted in an impairment of EA production in both cell lines compared to native cells (Table 3).

3.8. Membrane cholesterol and PKC activity

The role of PKC in the process of EBV entry and EA production is well known [14]. We calculated the enzyme activity in the membrane and cytosol compartment of Raji and Akata cells with or without cholesterol enrichment. The calculated enzyme activity has been reported in Table 4. After induction with the tumor promoter and PKC activator TPA, no effect of cholesterol on PKC activity was detected in both cell lines.

3.9. Effect of membrane cholesterol on PKC dependent protein phosphorylation

Fig. 5A shows a typical autoradiograph from Akata cell lysate (control cells) of the electrophoretic analysis of the phosphorylated species resolved in two-dimensional gel. Cell membrane enrichment with cholesterol resulted in a decrease in the incorporation of ^{32}P in some phosphoprotein (Fig. 5C), those phosphoproteins are specifically phosphorylated by PKC as reported in Fig. 5B and D where the phosphorylation was carried out in presence of protein kinase C activator TPA or in the presence of the protein kinase C inhibitor Bisindolylmaleimide. The same results were obtained when Raji cells were used instead of Akata.

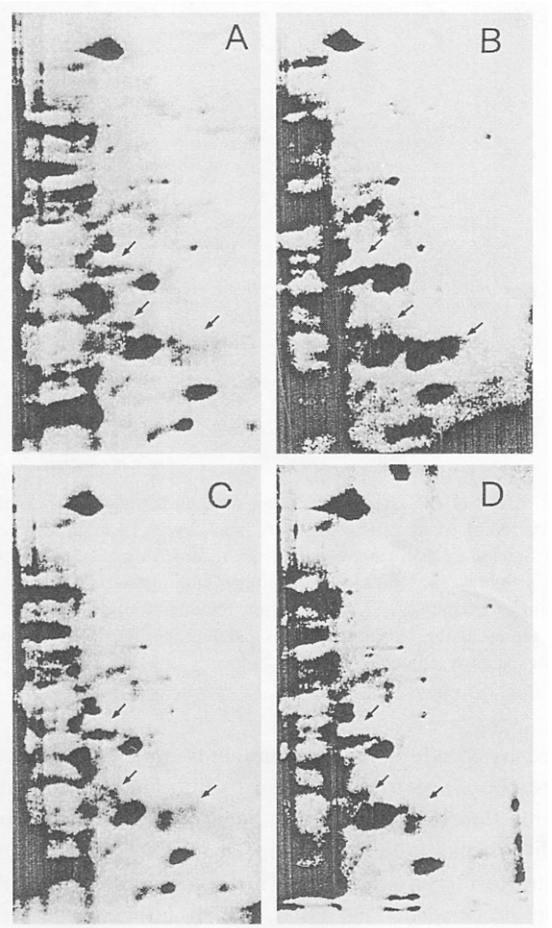

Fig. 5. Effect of membrane cholesterol on PKC dependent protein phosphorylation. Control (A), TPA induced (B), cholesterol enriched and TPA induced (C) and bisindolylmaleimide treated and TPA induced (D) Akata cells preincubated with ^{32}P. Cells homogenate were separated by charge in the first dimension and in SDS PAGE in the second dimension. Autoradiograph of the gel shows labelled spots (arrow) corresponding to proteins specifically phosphorylated by PKC.

Table 4
PKC activity in cytosol and particulate fractions of Raji and Akata cells cholesterol enriched

Treatment	PKC activity (pmol/min/mg protein)	
	cytosol	particulate
Raji control	364 ± 12 [a]	400 ± 19
Raji cholesterol	390 ± 11	395 ± 21
Akata control	402 ± 10	380 ± 20
Akata cholesterol	400 ± 10	395 ± 12

After cells lysis assay were carried out with the 0.2 M NaCl fraction eluted from DEAE-Sepharose column as described under Section 2.
[a] mean ± S.D.

4. Discussion

Membrane fusion is a complex phenomenon involving a wide range of biochemical and biophysical interaction [30]. Factors which govern membrane–membrane interaction such as the role of lipid structure, head group, shape, hydration have been studied deep inside [31,32]. Enveloped animal viruses infect cells injecting their nucleocapsid into the host cell. The key to this strategy is membrane fusion, either at the plasma membrane or within the endocytic vesicles [33]. The fusogenicity of the enveloped virus to target cell membrane has been studied using normal cells and liposomes with different lipid composition [34–36]. In these studies the hypothesis that the

lipid moiety is important in virus receptor recognition and fusion is evident, although little is known about the mechanism by which lipid can regulate virus fusion. Cholesterol seems to modulate the fusion process of several viruses. For example binding and fusion of Semliki Forest virus [33] and Sendai virus [37], require cholesterol in the target membrane. Patel [36] suggested that cholesterol can be of same importance in regulating EBV fusion. The mechanism leading to EBV fusion with its target membrane is a process that despite its complexity has been described at molecular level [12,13]. Immediately after binding of the viral gp 350/220 to the CR2 molecule, fusion is then induced by a third viral protein the gp 85.

EBV fusion with cells containing the EBV genome latently expressed (superinfection) results in the induction of the latent viral DNA. In this event PKC plays a central role, since phosphorylation of nuclear protcins is needed to trigger EBV replication [14].

Indirect immunofluorescence using anti CR2 monoclonal antibodies (OKB-7), specific for a protein sequence near the EBV binding domain, showed Akata cells are less positive than Raji. This is quite intriguing since Akata cells are known to be more susceptible to EBV infection, as also reported in the fusion kinetics with R18 label EBV and EA production. Since enrichment of Akata cell membranes with cholesterol succinate drastically reduces both fusion and EA induction, it is possible to argue that modification of some properties of the plasma membrane due to cholesterol can interfere with EBV infection.

The relevance of cholesterol for structural and dynamic properties of the majority of cell membrane in eucaryotic cells is well recognized [28]. The influence of cholesterol on the properties of phospholipid bilayers at a molecular level has been ruled out using several spectroscopic technique. Membrane fluidity is modified by cholesterol inducing to a more disordered gel phase while the liquid crystalline is ordered [38].

Single cell Laurdan emission generalized polarization identified on Raji two populations typical of fluid and rigid membrane respectively. When the same experiment was repeated on Akata cells, Laurdan emission generalized polarization generated a single population in the GP range from 0.35 to 0.25 typical of fluid membranes. Incubation of Akata cells with cholesterol succinate shifted the GP values of each single cells towards values corresponding to more rigid structures. Since this increase in Laurdan GP can be interpreted as a decrease in membrane fluidity (rigidification), it is possible to argue that cholesterol is rigidifies Akata plasma membranes. We also attempted to quantify membrane viscosity using a fluorophore different from Laurdan: DPH and TMA-DPH. Such probes monitor membrane fluidity through their sensitivity to the polarized light, have high extinction coefficients and are not fluorescent in water. Two probes were used because the ionic properties of TMA-DPH allow for it to report on the motional characteristic of the exofacial leaflet of the plasma membrane. Polarization values using DPH and TMA-DPH suggested significantly greater hindrance of the probes mobility in Raji and in cholesterol enriched Akata at all temperature measured than showed by control Akata cells. This is consistent with the data obtained by Laurdan emission GP and is in accordance with the greater cholesterol/phospholipid molar ratio found in Raji as compared to Akata.

On the other end looking at % EA positive Akata cells and GP values from single native and cholesterol enriched Akata cells, it can be withdrawn that more rigid is the membrane (higher GP values), less inducible is the cell.

It is surprising that Akata cells which are less positive by CR2 indirect immunofluorescence than Raji, are more inducible by EBV superinfection. There is a close correlation between membrane fluidity, EBV fusion and EA production. Above a critical GP value characteristic of most of the Raji population and cholesterol enriched Akata cells, the virus is not able to fuse with its receptor and EA induction is blocked.

In accord with Patel [16] we also found that the amount of virus bound was not affected by the presence of cholesterol (data not shown). This implies that fusion and not binding is the first in the cascade leading to EA production after superinfection.

The mechanisms leading to disruption of EBV latency is initiated by the expression and activation of a nuclear protein called ZEBRA (Z Epstein Barr Replicator Activator), a phosphoprotein whose function at the nuclear level is regulated by phosphorylation. Phosphoprotein analysis on native and cholesterol enriched cells demonstrated that together with the increase in membrane fluidity there is an impairment in the PKC dependent protein phosphorylation (Fig. 5).

Since we demonstrated previously [14] that as a consequence of EBV binding there is PKC translocation and increase in membrane protein phosphorylation, it seems reasonable to conclude that the failure for EBV to trigger EA production in superinfected cholesterol enriched Akata cells, can be related to an impairment in the phosphorylation of nuclear protein important for the EBV genome activation.

Acknowledgements

We wish to thank Dr. Delio Mercanti for his scientific and technical support. This work was partially supported by the 'Progetto finalizzato C.N.R FATMA' #104299/41/9409652 and by the Associazione Nazionale Ricerca sul Cancro 'AIRC'.

References

[1] Klein, G. (1988) Advances in Viral Oncology, Vol. 8, Raven Press, New York.

[2] Epstein, M.B., Achong, A.N. and Barr, Y. (1964) Lancet 1, 702–703.
[3] Baichwall, V. and Sudgen, B. (1988) Cell 52, 702–703.
[4] Faggioni, A., Z4ompetta, C., Grimaldi, S., Barile, G., Frati, L. and Lazdins, J. (1986) Science 232, 1554–1556.
[5] Lazdins, J., Zompetta, C., Grimaldi, S., Barile, G., Venanzoni, M., Frati, L. and Faggioni, A. (1987) Int. J. Cancer 40, 846–849.
[6] Cirone, M., Angeloni, A., Barile, G., Zompetta, C., Venanzoni, M., Torrisi, M.R. and Frati, L. (1990) Int. J. Cancer 45, 490–493.
[7] Henle, W., Henle, G., Zajac, B., Pearson, G., Waubke, R. and Scriba, M. (1970) Science 169, 188–190.
[8] Fingeroth, J., Weis, J., Tedder, T., Strominger, J., Bird, P. and Fearon, D. (1984) Proc. Natl. Acad. Sci. USA 81, 4510–4516.
[9] Nemerow, G.R., Mold, C., Schwenid, V.K., Tallefson, V. and Cooper, N.R. (1987) J. Virol. 61, 1416–1442.
[10] Wells, A., Koide, N. and Kleine, G. (1982) J. Virol. 41, 286–297.
[11] Tanner, J., Weis, J., Fearon, D., Whang, Y. and Kieff, E. (1987) Cell 50, 203–213.
[12] Pozzi, D., Zompetta, C., Faggioni, A., Lisi, A., De Ros, I., Ravagnan, G. and Grimaldi, S. (1990) Membr. Biochem. 9, 2392–2451.
[13] Miller, N.M. and Hutt-Fletcher, L.M. (1992) J. Virol. 66, 3409–3414.
[14] Aquino, A., Lisi, A., Pozzi, D., Ravagnan, G. and Grimaldi, S. (1993) Biochem. Biophys. Res. Commun. 196, 794–802.
[15] Cheetham, J.J., Epand, R.M., Andrews, M. and Flanagan, T. (1990) J. Biol. Chem. 265, 12404–12409.
[16] Patel, R.A., Hutt-Fletcher, L.M. and Crews, F.T. (1993) Virology 195, 121–131.
[17] Chong, P.L.G. (1990) High Pressure Res. 5, 761–763.
[18] Lisi, A., Pozzi, D. and Grimaldi, S. (1993) Membr. Biochem. 10, 203–212.
[19] Parasassi, T., Conti, F. and Gratton E. (1986) Cell Mol. Biol. 32, 103–108.
[20] Parasassi, T., De Stasio, G., Ravagnan, G., Rusch, R.M. and Gratton, E. (1991) Biophys. J. 60, 179–189.
[21] Bligh, E.G. and Dyer, W. (1959) Can. J. Biochem. Phisiol. 37, 911–917.
[22] Zlatkis, A., Zak, B. and Boyle, A.J. (1953) Lab. Clin. Med. 41, 486–492.
[23] Pal, R., Barenholz, Y., and Wagner, R.R. (1981) Biochemistry 20, 530–539.
[24] Heron, D., Shinitzky, M., Hershkowitz, M. and Samuel, D. (1980) Proc. Natl. Acad. Sci. USA 12, 7463–7467.
[25] Eboli, M.L., Mercanti, D., Ciotti, M.T., Aquino, A. and Castellani, L. (1994) Neurochem. Res. 10, 1257–1264.
[26] Laemmli, U.K. (1970) Nature (London) 227, 680–685.
[27] Pozzi, D., Faggioni, A., Zompetta, C., De Ros, I., Lio, S., Lisi, A., Ravagnan, G., Frati, L. and Grimaldi, S. (1992) Intervirology 33, 173–179.
[28] Parasassi, T., Di Stefano, M., Loiero, M., Ravagnan, G., and Gratton, E. (1994) Biophys. J. 66, 763–768.
[29] Prendergast, F.G., Haugland, R.P. and Callahan, P.J. (1981) Biochemistry 20, 7333–7338.
[30] Blumenthal, R., Puri, A., Walter, A. and Eidelman, O. (1987) In Molecular Mechanisms of Membrane Fusion (Shinpei Ohki, ed.), pp. 367–383, Plenum Press, New York.
[31] Puri A., Grimaldi, S. and Blumenthal R. (1992) Biochemistry 31, 10108–10113.
[32] Blumenthal, R., Puri, A., Sakar, D.P., Yi-der Chen, Eidelman O., and Morris S.J. (1989) Cell Biology of virus entry, replication and pathogenesis, pp. 197–217, Alan R. Liss.
[33] White, J., KIelian, M. and Helenius, A. (1983) Q. Rev. Biophys. 16, 151.
[34] Hoekstra, L., Klappe, K., De Boer, T. and Wilschut, J. (1985) J. Biochem. 24, 4739–4745.
[35] Moore, N.F., Patzer, E.J., Shaw, J.M., Thompson, T.E., and Wagner, R.R. (1978) J. Virol. 27, 320–325.
[36] Patel, R.A., Hutt-Fletcher, M.L. and Crews, F.T. (1993) Virology 195, 121–131.
[37] Hsu, M.C., Scheid, A. and Choppin, P.W. (1983) Virology 126, 361–369.
[38] Vist, M.R. and Davies, D.J. (1990) Biochemisty 29, 451–464.